V European Conference on Computational Fluid Dynamics
ECCOMAS CFD 2010
J. C. F. Pereira and A. Sequeira (Eds)
Lisbon, Portugal,14-17 June 2010

RECONSTRUCTING EXPERIMENTAL DATA FROM VIDEO RECORDS FOR FILM OVER A SPINNING DISK

Valentina N. Korzhova[†], Dmitry B. Goldgof[†] and Grigori M. Sisoev[††]

[*]University of South Florida,
4202 E. Fowler Ave. Tampa, Florida 33620, USA
e-mail: {korzhova@cse.usf.edu, goldgof@cse.usf.edu }
[†]School of Mathematics
University of Birmingham Birmingham B15 2TT, UK
e-mail: {G.Sisoev@bham.ac.uk}

Key words: Fluid Dynamics, Stationary Spiral Waves, Wave Detection, Wave Tracking

Abstract. *New non-invasive method to obtain quantitative information about wave regimes from recorded videos has been developed and utilized on numerous video sequences. The videos were recorded using an experimental set-up with a spinning disk whose rotational speed as well as flow rate of water pouring onto a disk were controlled.*

Particular attention was paid to stationary spiral waves observed on the film surface at relatively large flow rates. Analysis of numerous videos allowed us to conclude that the observed spiral waves are approximated by the Archimedean spirals whose coefficients depend on the Eckman number. Experimental results are in a good agreement with numerical results obtained from a new evolution model describing film flow over a spinning disk.

1 INTRODUCTION

The flow of a liquid film over a rapidly rotating horizontal disk has numerous industrial applications (pharmaceutical, chemical engineering, bioengineering, etc.), ranging from spin-coating of silicon wafers to the atomization of liquids. One of the most important applications is the absorption of gases, such as carbon dioxide, by the flowing film. The film flows are accompanied by formation of non-linear waves, leading to remarkably large increases of heat and mass transfer. Therefore, the analysis and control of film flow over a rapidly rotating horizontal disk is a major scientific problem.

The experimental studies [2, 23] have shown that the presence of surface waves leads to significant enhancement of the transfer processes at the film surface. The film flow over a spinning disk demonstrates that various wave regimes affect the mass/heat transfer intensity [2]. If the flow rate is relatively small, the film surface is smooth [2, 3, 4, 7, 12, 23]. With its increase at given values of other physical parameters, circumferential waves appear traveling from the disk center to its periphery. Nonaxisymmetric wave structures are observed at greater flow rates [23]. Stationary spiral waves unwinding in the direction of rotation have been observed at different values of the flow rate [4, 7, 12, 23].

Axisymmetric flow regimes have been studied experimentally and theoretically in many works [13] examining the waveless flow [4, 16, 18] and its linear stability [4, 19, 20]. Recently, progress in modeling nonlinear axisymmentric wave regimes has been achieved in the framework of evolutionary equations derived in [21]. On the other hand, non-axisymmetric flow regimes [4, 12] have not been explained theoretically.

Using videos, a motion analysis of non-rigid objects has received significant attention over the last two decades [6, 9]. Having initially been developed for articulated and elastic motion [1, 8], analysis of fluid-like motions has also been attempted [6, 10, 11, 24].

In this paper, we develop a special experimental and computational technique to study the non-axisymmetric flows in the form of the stationary spiral waves. To model the waves, we have generalized the evolution equations [21] for non-axisymmetric flows. In the cases when the capillary forces might be omitted, stationary solutions have been analyzed.

The recorded videos provides no impact at the film flow. The developed method allowed us to drastically simplify the set-up in comparison with mechanical [7, 14], electrical [15, 17] or optical [4, 23] methods, which use supplementary devices and use image analysis to process experimental data.

The rest of the paper is organized as the following. In Section 2 the experimental set-up is described and algorithms of wave detection, tracking, and estimation of fluid-flow parameters are presented. Numerical results and their comparison with theoretical data are presented in Section 3, followed by conclusions provided in Section 4.

2 EXPERIMENTAL SET-UP AND WAVE TRACKING FROM VIDEOS

The experimental set-up consists of: a motor, aluminum flat/round stock, reservoir, tubing, brass adapters, bunged cords, flow-meter, copper tubing, aluminum control box,

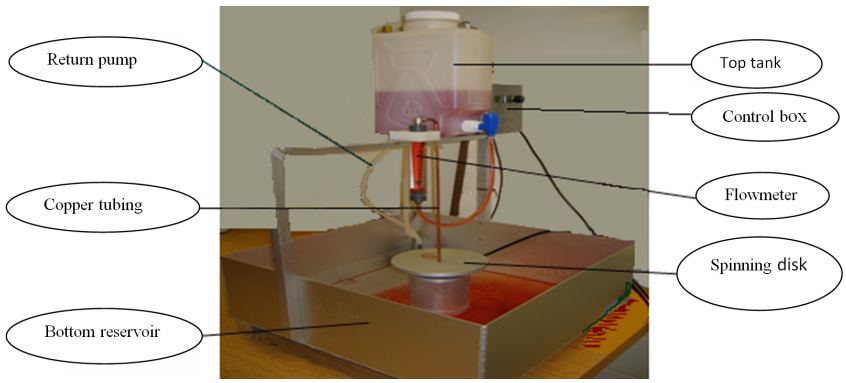

Figure 1: Set-up of experiment.

switches, return pump, miscellaneous hardware (Figure 1). The main characteristic of the motor (PWMDC Motor Speed Control Module 6-15V/24A)is given by the turnable calibration. Measurements were performed in the following way. Water contained in a plastic container with an adjustment valve for the flow was drained through the copper tubing at a constant starting flow rate Q, which can be changed in the range of 0.2-0.8 lpm (liter per minute). Liquid emerged from the nozzle as a free jet pouring out onto the center of a constantly rotating aluminum disk with a diameter of 200 mm. The rotational frequency of the disk was monitored by a motor control. Water leaving the rotating disk was collected at the bottom reservoir and recycled to the top reservoir by a pump.

At all flow rates and spinning velocities the film surface was covered with waves whose parameters were calculated from videos recorded with a portable camcorder Canon Optura 20 capable of capturing images at 30 fps (frames per second) and shutter time of $1/2000th$ sec and with high definition camera(JVC GY-HD 100), capable of capturing images at 30 fps (resolution 1280x720, color). Before systematic recording for the following processing, preliminary installations of the camera and light sources had been carried out to achieve a better quality of videos. Example of a flowing film covered by spiral waves is shown in Figure 2.

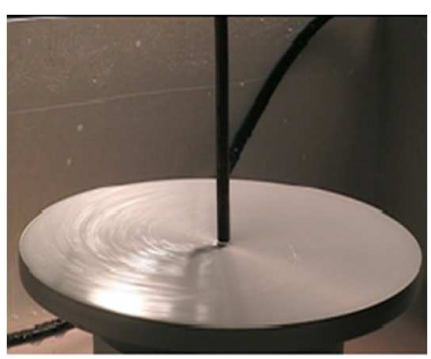

Figure 2: Film surface in the case $\Omega = 300$ rpm, $Q_c = 0.4$ lpm.

Sixty videos were collected for different regimes of the film flow and disk rotation. Fifteen videos were taken with the flow rate of 0.8 lpm and the disk rotation of 300 rpm, fifteen videos were taken with the flow rate of 0.4 lpm and the disk rotation of 500 rpm, and the rest of them with different flow rates and different disk rotations.

Prior to video recording calibration of the camera was performed by using a square pattern placed on the surface of the disk. Camera calibration is a necessary step in computer vision analysis in order to extract metric information from 2D images and then reconstruct real objects with given accuracy [5, 25]. The recalculation technique in the form of a closed-form solution followed by a nonlinear refinement has been applied. This technique was built in the developed algorithm in order to calculate actual values from the frame values measured in pixels.

The works [10, 11] focus on developing a novel approach for fluid flow tracking and analysis. Specifically, the developed algorithm is able to detect the moving waves and compute physical film flow parameters for the fluid flowing over a rotating disk. The input to this algorithm is an easily acquired non-invasive video data.

It is shown [11] that under a single light illumination it is possible to track specular portion of the reflected light on the moving wave. Hence, the fluid wave motion can be tracked and the fluid flow parameters can be computed (see Figure 3). It is also shown

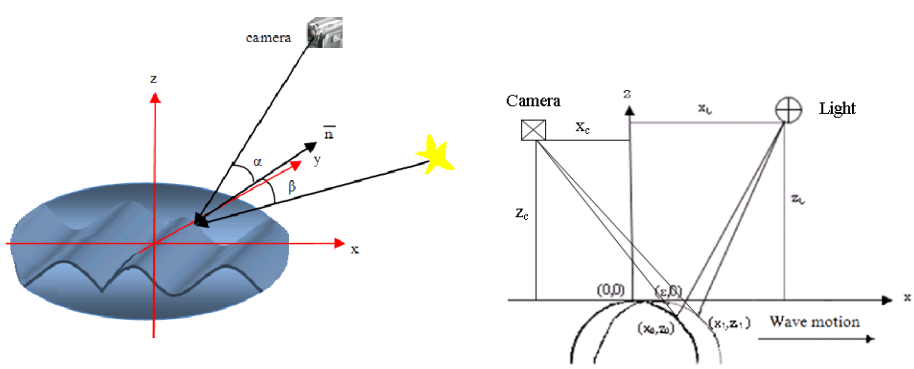

(a) (b)

Figure 3: (a) The incident angle α and the emittance angle β; (b) A camera and light are in the different locations, $\frac{x_c}{z_c} \leq \epsilon$.

that under general camera and light positions, the specular points do not coincide with the peaks of the waves. However, the distances along the radial direction between the specular points and the peaks are approximately constant for the moving wave. Hence, tracking the specular points allows us to track the wave of fluid flowing over a rotating disk.

Prior to the process of detecting the points on the waves, preprocessing of images is performed. The points at which the positive direction of intensities changes to the negative

direction are detected. Let Δr be the radius-step in the polar system coordinates, and

$$(\phi_i, k\Delta r; I_{ik}), \quad i = 1, 2, ..., N; \quad k = 1, 2, ..., \tag{1}$$

be the detected points on the observed disk, where N is the number of the observed radius-vectors and I_{ik} are the intensities of the points $(\phi_i, k\Delta r)$. Then $R_{ij} = k_j \Delta r$, where I_{ik_j} is $j-th$ maximum of intensities I_{ik}, $j = 1, 2, ..., S$; S is the number of spirals for each i.

The values $R_{ij}, \quad i = 1, ..., N, \quad (5-10) \quad j = 1, ..., S, \quad (10-14)$ are given data points on the observed disk in the standard form of ellipsis with the parameters $a = R$ and $0 < b < R$. Their nominal values in the original disk of 3-D space are:

$$\begin{aligned} & r_{ij} = r_j(\phi_i) = R_{ij} \frac{R}{[(a\cos\phi_i)^2 + (b\sin\phi_i)^2]^{1/2}}, \\ & \phi_0 = 0, \quad \phi_i = i\Delta\phi, \quad i = 1, ..., N, \\ & j = 1, ..., S, \end{aligned} \tag{2}$$

where$\Delta\phi$ is the angle step in the polar system coordinates and R is the radius of the disk. Considering the spiral waves as periodic functions due to their stationary properties [12] with respect to the rotating disk, the tracked spirals are:

$$\begin{aligned} & 1^{st} spiral: \quad (\phi_1, r_{11}), \quad ..., \quad (\phi_N, r_{N1}); \\ & (\phi_{N+1}, r_{12}), \quad ..., \quad (\phi_{2N}, r_{N2}); \quad ... \quad ; \\ & (\phi_{(S-1)N+1}, r_{1S}), \quad ..., \quad (\phi_{SN}, r_{NS}); \\ & .....; \\ & (n+1)^{th} spiral: (\phi_{nN+1}, r_{11}), ..., (\phi_{(n+1)N}, r_{N1}); \\ & (\phi_{(n+1)N+1}, r_{12}), \quad ..., \quad (\phi_{(n+2)N}, r_{N2}); \quad ...; \\ & (\phi_{(n+S-1)N+1}, r_{1S}), \quad ..., \quad (\phi_{(n+S)N}, r_{NS}). \end{aligned}$$

This process has been continued for all frames and repeated for each video sequence. Samples of resulting images are shown in Figure 4.

The estimate of the radial velocity component is given by

$$r'_{exp} = \frac{\Delta r}{\Delta t} = \frac{r_{t_{i+1}} - r_{t_i}}{\Delta t}, \quad \Delta t = |t_{i+1} - t_i|, \tag{3}$$

where r_t and r_{t+1} are the values of the radii from the center to the points on the wave at the moments t_i and t_{i+1}. And the estimate of the inclination angle is given by

$$\tan\beta = \frac{1}{\tilde{r}} \frac{d\tilde{r}}{d\theta} \approx \frac{1}{r} \frac{r(\theta + \Delta\theta) - r(\theta - \Delta\theta)}{2\Delta\theta}. \tag{4}$$

The problem of estimating the inclination angle β and the radial velocity component $r'_e xp$ is ill-posed. So, the asymptotically optimal method for minimizing error of estimate under a known error of initial data was used.

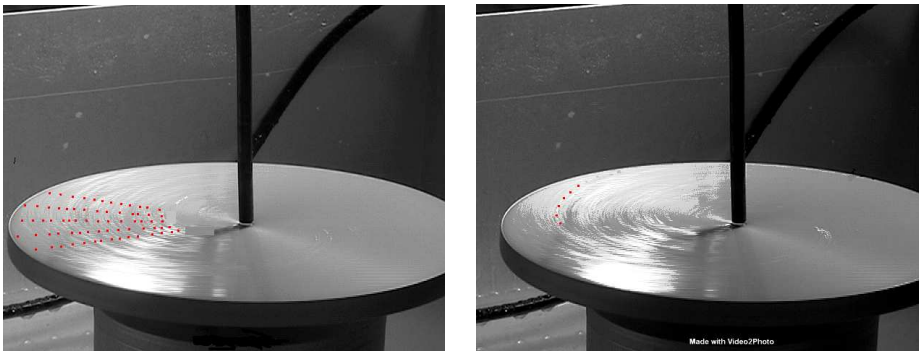

(a) (b)

Figure 4: (a) Detected Points of Waves. (b) A detected wave.

3 RESULTS

In this section we present experimental results about the spiral waves on the film surface.

The video sequences of fluid flow over a rotating disk of 500 *rpm* and the flow rate of 0.8 *lpm* are used to calculate average wave inclinations. The results for ten videos (taken with camera Optura) are illustrated in Table 1. The results for five videos (taken with

Table 1: Experimental wave inclinations (in radian). Video data are taken using camcorder Optura 20.

Radii (in mm) / *Video numbers*	40	50	60	70	80	90	100
1	1.01	0.73	0.54	0.47	0.36	0.34	0.30
2	0.97	0.73	0.53	0.46	0.36	0.33	0.3
3	0.96	0.7	0.5	0.45	0.35	0.32	0.28
4	1.01	0.73	0.54	0.47	0.34	0.32	0.29
5	0.96	0.71	0.5	0.43	0.33	0.31	0.28
6	1	0.72	0.54	0.44	0.35	0.34	0.3
7	0.96	0.71	0.5	0.45	0.33	0.33	0.29
8	0.97	0.73	0.51	0.44	0.35	0.31	0.29
9	0.99	0.69	0.5	0.43	0.33	0.31	0.28
10	0.96	0.71	0.52	0.47	0.35	0.34	0.3
Average	0.979	0.716	0.518	0.451	0.346	0.325	0.291
Standard deviation	0.021	0.014	0.018	0.016	0.011	0.013	0.009

High Definition camera) are illustrated in Table 2. The video sequences of fluid flow over a rotating disk of 500 *rpm* and the flow rate of 0.8 *lpm* are used to calculate average wave inclinations.

Table 2: Experimental wave inclinations (in radian). Video data are taken using high definition camera (JVC GY-HD 100).

Radii (in mm) / *Video numbers*	40	50	60	70	80	90	100
1	0.97	0.72	0.53	0.47	0.36	0.33	0.28
2	1.01	0.72	0.52	0.43	0.34	0.32	0.3
3	0.98	0.71	0.5	0.45	0.36	0.32	0.28
4	1.0	0.70	0.52	0.44	0.35	0.33	0.29
5	0.94	0.72	0.49	0.45	0.36	0.31	0.30
Average	0.98	0.714	0.512	0.448	0.354	0.322	0.29
Standard deviation	0.027	0.009	0.016	0.015	0.009	0.008	0.01

As seen from Tables 1 and 2, the high definition camera does not improve the accuracy of estimations of the film flow parameters.

The angle characterizing the spiral deviation off of a circle is

$$\beta \equiv \arctan\left(\frac{1}{r}\frac{dr}{d\theta}\right). \tag{5}$$

In the case of the spiral,

$$\beta \equiv \arctan\left(\frac{1}{r}\frac{dr}{d\theta}\right) = \arctan\left(\frac{\alpha\,(\mathrm{E})}{r}\right),$$

and thus

$$E = \frac{\nu}{\Omega H_c^2},$$

where

$$H_c = \left(\frac{Q_c \nu}{2\pi\Omega^2 R_c^2}\right) 1/3,$$

and R_c is the radius scale of the flow. The dependence $\alpha(E)$ has been theoretically revealed.

The coefficient α, as shown in [22], depends on Eckman number. The values of inclination angles and the polar coordinates of detected wave are given in Table 3 in the case of the disk speed (Ω) 400 *rpm* and film flow rate (Q) 0.4 *lpm*.

Fig. 5 shows experimental values of the spiral angle depending on radius in five experimental cases.

Fig. 6 shows the experimental dependence $\tan\beta$ of radius $\tilde{r}$ and its approximation by the dependence in the form $\tan\beta = \frac{\alpha}{\tilde{r}}$.

Table 3: Polar coordinates and experimental wave inclinations (in radian).

Radius (in mm)	*Azimuthal angle*	*Inclination angle*
40	π	1.41
45	0.92π	1.36
50	0.85π	1.32
55	0.78π	1.23
60	0.71π	1.14
65	0.65π	1.1
70	0.57π	1.00
75	0.51π	0.95
80	0.45π	0.90
90	0.37π	0.89

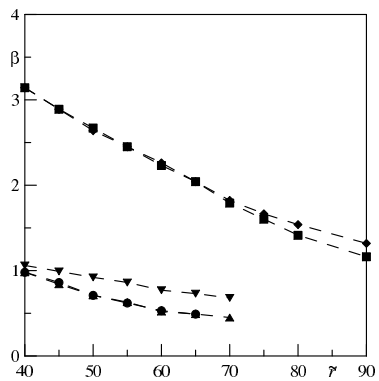

Figure 5: Spiral angles vs radius in five experimental cases ($\bullet$ $\Omega = 500$, $Q = 0.8$; $\diamond$ $\Omega = 300$, $Q = 0.4$; Π $\Omega = 400$, $Q = 0.4$; $\triangle$ $\Omega = 800$, $Q = 0.8$; ∇ $\Omega = 600$, $Q = 0.6$.)

To compare the theoretical curve with experimental data, we suggested that a theoretical value of the angle β meets the experimental value β_{exp} at the maximum radius, $\tilde{r}_{max}$ i.e.

$$\tan \beta_{exp} = \frac{\alpha\,(\mathrm{E})\,R_c}{\tilde{r}_{max}}.$$

This equation allowed us to find the free parameter R_c to denote the experimental data in Fig. 6. It is seen that the theoretical curve is in a good agreement with the experimental data at relatively large radii. The biggest deviation of the experimental and theoretical results is at the smallest value of radius where the solution is strongly affected by the inlet flow conditions.

The simple relation, $r = \alpha\,(\mathrm{E})\,(\theta - \theta_0) + r_0$, describes spiral waves at the Eckman

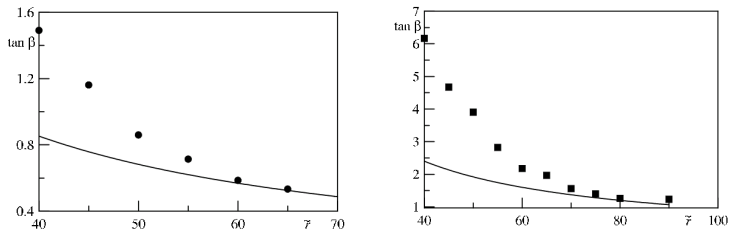

(a) (b)

Figure 6: (a) Solid curve and full dots correspond to theoretical and experimental values at $\Omega = 500\ rpm$, $Q_c = 0.8\ lpm$ with E = 1.19 and $\alpha = 1.75$. (b) Solid curve and full squares correspond to theoretical and experimental values at $\Omega = 400\ rpm$, $Q_c = 0.8\ lpm$ with E = 3.11 and $\alpha = 3.7$.

numbers when the waves are clearly observed. For instance, theoretical values calculated by using the approximation [22] are in a good agreement with the experimetal data.

4 CONCLUSIONS

This paper presents a novel video-based algorithm to detect moving waves and to determine quantitative information about wave regimes. The input to this algorithm is an easily acquired non-invasive video data, recorded using an experimental set-up with a spinning disk whose rotation speed as well as flow rate of water pouring onto the disk were controlled. The data was processed from the recorded videos by using image processing analysis.

It has been shown that stationary spiral waves observed in film flow over a spinning disk are accurately approximated by the Archimedean spirals whose coefficient depends on the Eckman numbers. The explicit formula allowing us to find the Archimedean spiral's coefficient at relatively small Eckman numbers was received. The experimental results are in a good agreement with the theoretical predictions.

REFERENCES

[1] K. Aggarwal, Q. Cai, W. Liao, and B. Sabata, "Nonrigid motion analysis - articulated and elastic motion (review)," Computer Vision and Image Understanding **70**, 142 (1998).

[2] A. Aoune and C. Ramshaw, "Process intensification: heat and mass transfer characteristics of liquid films on rotating discs," Int. J. Heat Mass Transfer **42**, 2543 (1999).

[3] A. I. Butuzov and I. I. Puhovoi, "On regimes of liquid film flows over a rotating surface," Journal of Engineering Physics **31**, 217 (1976).

[4] A. F. Charwat, R. E. Kelly, and C. Gazley, "The flow and stability of thin liquid films on a rotating disk," J. Fluid Mech. **53**, 227 (1972).

[5] T. A. Clarke and J. G. Fryer, "The development of camera calibration methods and models," Photogrammetric Record **16(91)**, 51 (1998).

[6] T. Corpetti, E. Memin, and P. Perez, "Dense estimation of fluid flows," IEEE Transactions on Pattern Analysis and Machine Intelligence **24**, 365 (2002).

[7] H. Espig and R. Hoyle, "Waves in a thin liquid layer on a rotating disk," J. Fluid Mech. **22**, 671 (1965).

[8] D. B. Goldgof, H. Lee, and T. Huang, in *IEEE Conference on Computer Vision and Pattern Recognition* (IEEE Computer Society, Ann Arbor, Michigan, USA, 1988), pp. 899–904.

[9] C. Kambhamettu, D. B. Goldgof, D. Terzopoulos, and T. Huang, in *Computer Vision, Handbook of Pattern Recognition and Computer Vision* (Academic Press, San Diego, USA, 1994), Vol. 2, Chap. 11.

[10] V. N. Korzhova, D. B. Goldgof, and G. M. Sisoev, in *Proceedings of the 18th International Conference on Pattern Recognition* (IEEE Computer Society, Hong Kong, 22-24 August, 2006), Vol. 1, pp. 396–399.

[11] V. Korzhova, D. Goldgof, and G. Sisoev, in *Optical 3-D Measurement Techniques IX* (World Scientific Publishing Company, Vienna, Austria, 2009), pp. 231–240.

[12] G. Leneweit, K. G. Roesner, and R. Koehler, "Surface instabilities of thin liquid film flow on a rotating disk," Experiments in Fluids **26**, 75 (1999).

[13] O. K. Matar, G. M. Sisoev, and C. J. Lawrence, "The flow of thin liquid films over spinning discs," Canadian Journal of Chemical Engineering **84**, 625 (2006).

[14] S. Matsumoto, K. Saito, and Y. Takashima, "The thickness of a viscous liquid film on a rotating disk," J. Chem. Engng. Japan **6**, 503 (1973).

[15] Y. Miyasaka, "On the flow of a viscous free boundary jet on a rotating disk (2nd Report. Comparison of experimental results with calculated values by means of film thickness)," Bull. JSME **17**, 1469 (1974).

[16] J. W. Rauscher, R. E. Kelly, and J. D. Cole, "An asymptotic solution for the laminar flow of thin films on a rotating disk," J. Appl. Mech. **40**, 43 (1973).

[17] V. G. Rifert, P. A. Barabash, and A. A. Muzhilko, "Stochastic analysis of wave surface structure of liquid film flowing under centrifugal forces," High-School Bulletin, Power Engineering **(8)**, 62 (1982).

[18] G. M. Sisoev, A. F. Tal'drik, and V. Y. Shkadov, "Flow of a viscous liquid film on the surface of a rotating disc," Journal of Engineering Physics **51**, 1171 (1986).

[19] G. M. Sisoev and V. Y. Shkadov, "Flow stability of a film of viscous liquid on the surface of a rotating disc," Journal of Engineering Physics **52**, 671 (1987).

[20] G. M. Sisoev and V. Y. Shkadov, "Helical waves in a liquid film on a rotating disc," Journal of Engineering Physics **58**, 573 (1990).

[21] G. M. Sisoev, O. K. Matar, and C. J. Lawrence, "Axisymmetric wave regimes in viscous liquid film flow over a spinning disk," J. Fluid Mech. **495**, 385 (2003).

[22] G.Sisoev, D. Goldgof, and V. Korzhova. "Stationary spiral waves in film flow over a spinning disk," Experimental Physics (inpress).

[23] W. P. Woods, Ph.D. thesis, University of Newcastle upon Tyne, UK, 1995.

[24] L. Zhou *et al.*, "Tracking nonrigid motion and structure from 2D satellite cloud images without correspondences," IEEE Transactions on Pattern Analysis and Machine Intelligence **23**, 1330 (2001).

[25] Z. Zhang, "A flexible new technique for camera calibration," IEEE Transactions on Pattern Analysis and Machine Intelligence **22**, 1330 (2000).